

# Automated streak-seeding with micromachined silicon tools

Atanas Georgiev,<sup>a\*</sup> Sergey Vorobiev,<sup>b</sup> William Edstrom,<sup>b</sup> Ting Song,<sup>c</sup> Andrew Laine,<sup>c</sup> John Hunt<sup>b</sup> and Peter Allen<sup>a</sup>

<sup>a</sup>Department of Computer Science, Columbia University, New York, NY, USA, <sup>b</sup>Department of Biological Sciences, Columbia University, New York, NY, USA, and <sup>c</sup>Department of Biomedical Engineering, Columbia University, New York, NY, USA

Correspondence e-mail:  
atanas@cs.columbia.edu

Received 6 March 2006

Accepted 21 June 2006

This report presents a new approach to streak-seeding based on custom-designed silicon microtools. Experimental data show that the microtools produce similar results to the commonly used boar bristles. One advantage to using silicon is that it is rigid and can easily serve as an accurately calibrated end-effector on a micro-robotic system. Additionally, the fabrication technology allows the production of microtools of various shapes and sizes. A working prototype of an automatic streak-seeding system based on these microtools was built and successfully applied for protein crystallization.

## 1. Introduction

Structural genomics projects are aimed at determining the three-dimensional structures of a large number of proteins to help in the development of a new generation of therapeutic drugs. Despite recent impressive achievements in high-throughput (HTP) protein crystallography, there are still several bottlenecks which hold up the large-scale X-ray structure pipeline. One of the largest obstacles is the production of high-quality crystals suitable for data collection and structure solution by modern HTP software. In Phase 1 of the Protein Structure Initiative (PSI), the Northeast Structural Genomics Consortium (NESG) solved and deposited in the Protein Data Bank (PDB; <http://www.pdb.org>) 116 protein crystal structures from approximately 400 proteins that were screened for crystallization (Acton *et al.*, 2005). Similar crystallization and structure-determination success rates were reported by other structural genomics consortia (Lesley & Wilson, 2005; the statistics for other consortia can be obtained from the PDB).

Some of this loss can be alleviated by crystal-optimization techniques (Chayen & Saridakis, 2002) including variation of pH, chemical environment, protein/precipitant concentration ratio, temperature or seeding. For example, the NESG data showed that many of the proteins that crystallize poorly can be streak-seeded to yield better diffraction-quality crystals that in turn result in resolved protein structures. As another example, researchers utilized streak-seeding to go from microcrystals to larger diffraction-quality crystals to obtain the structure of LIR-2 (Willcox *et al.*, 2002). Enhancing throughput and increasing success rates are vital for the structural biology community to progress to solving more challenging structures. Seeding is one methodology to enhance the quality of crystals obtained from challenging proteins (Bergfors, 2003; Stura, 1999; Stura & Wilson, 1990).

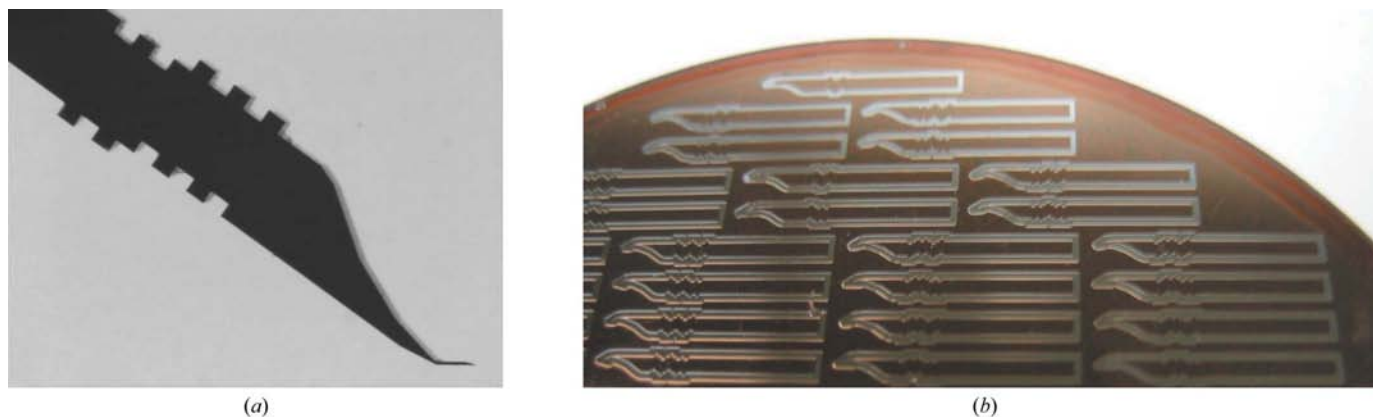


**Figure 1**  
(a) A sample microshovel; (b) microshovels during fabrication from a 100 mm wafer.

The protein structure initiative, started by the NIH (US National Institutes of Health; <http://www.nigms.nih.gov/psi>) in 1999 and extended into Phase 2 in 2005, accelerated the development of a diverse set of technologies for high-throughput protein production and three-dimensional structure determination. Many parts of the high-throughput pipeline have been either fully automated or have benefited by the introduction of robotic and automation technologies. However, streak-seeding remains a technique that has yet to be automated, even though it is an important part of the pipeline to obtain diffraction-quality protein crystals.

Streak-seeding is not a difficult task, but requires attention and concentration and takes up the valuable time of crystallographers and laboratory technicians. An automated solution would free up most of this time. Some manual work would still be needed to establish the conditions, but a robot could be used to explore these and, in our experience, streak-seeding a large plate (e.g. a 96-well plate) requires more human time than establishing solution conditions. Automation also minimizes the variability that exists between researchers and even from one seeding to another when the task is performed manually. Minimizing variability translates into greater reproducibility as well as more successful outcomes.

At first glance, the streak-seeding procedure appears to be simple, straightforward and an easy target for automation. However, it does present significant technical challenges.

Firstly, obtaining reliable sensory feedback on the microscale is difficult. Existing micro- and nano-force sensors, for example, have a short operating range for which they need to be tuned and many are still in the experimental stage. Secondly, the detection and location of protein crystals are challenging problems. Computer vision methods have been suggested and are still being improved (Saitoh *et al.*, 2004; Xu *et al.*, 2006; Wang *et al.*, 2005). Finally, conventional materials used for streak-seeding, such as various types of whiskers, hairs and bristles, are too soft and flexible and would require sophisticated tracking and visual servoing methods.

This report describes the automation and advancement of the streak-seeding methodology to overcome a major rate-limiting barrier to obtaining diffraction-quality crystals. We propose the use of silicon-made microtools in place of the prevalently used hairs, whiskers, bristles or other materials (D'Arcy *et al.*, 2003). We describe the manufacturing process of the microtools and present experiments demonstrating that they produce comparable results to the alternatives. However, the advantage of using silicon is twofold: it allows the use of existing state-of-the-art micro-electromechanical systems (MEMS) technology to manufacture microtools of various desired shapes and sizes and it is a rigid material that can easily serve as an accurately calibrated end-effector in a micro-robotic system. We have demonstrated this by building an autonomous streak-seeding prototype system, which we also describe here.

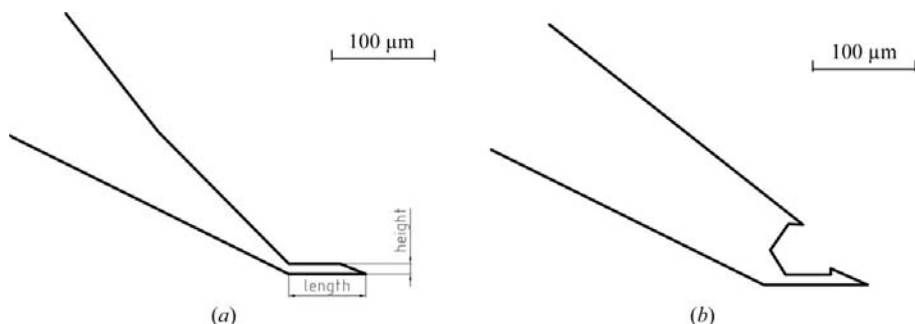


**Figure 2**  
Two different forms of silicon microshovels. (a) Design No. 0, (b) design No. 17A.

## 2. Materials and methods

### 2.1. Silicon microtools

The automatic streak-seeding procedure that has been developed is based on custom-made microtools called microshovels fabricated from a single-crystal silicon wafer (Fig. 1). The microshovels were designed and drawn using the *AutoCAD* software package (Autodesk). More than 30 different

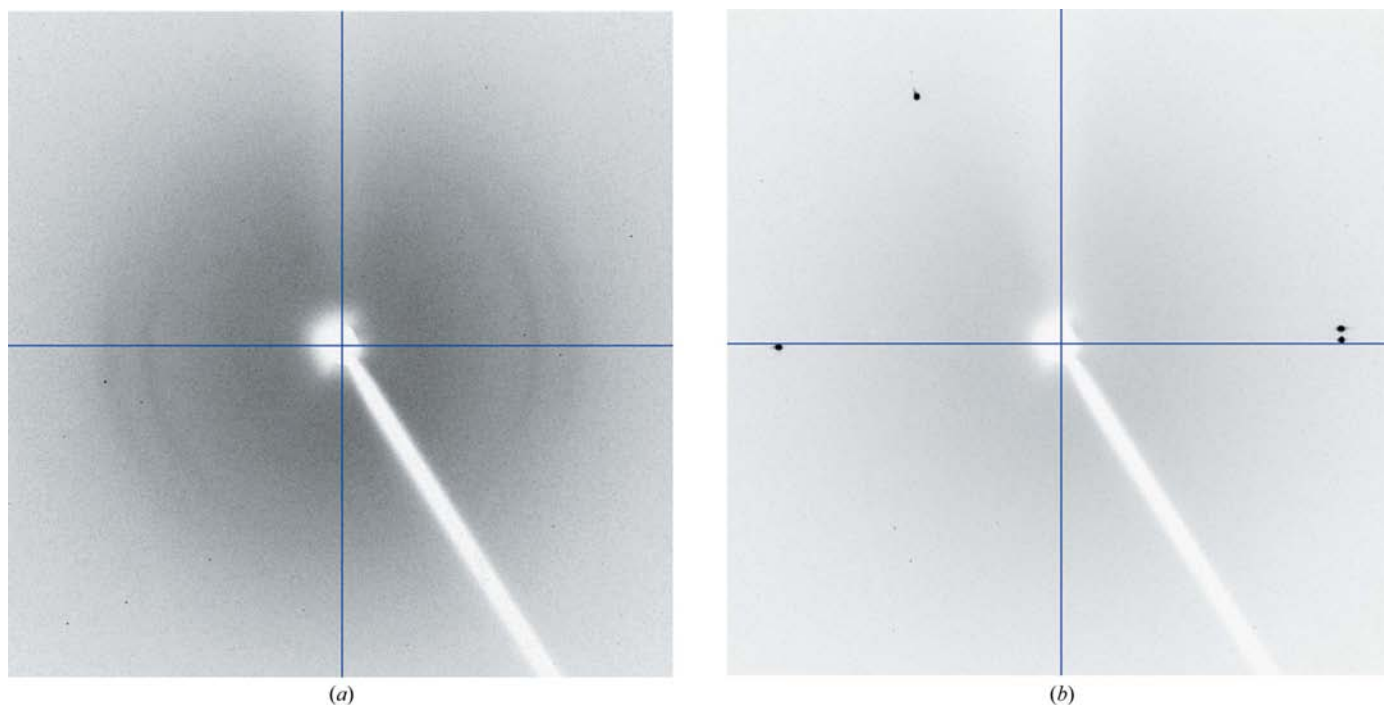


**Figure 3**  
X-ray diffractograms. (a) Empty 10  $\mu\text{m}$  Hampton Research CryoLoop; (b) empty silicon microshovel.

types of microshovels that differed in the shape and the size of their tooltips were designed. The tooltip shapes (Fig. 2) were also conceived with an additional application in mind: crystal mounting (Georgiev *et al.*, 2004). One advantage the microshovels have over nylon loops, which are typically used for mounting and X-ray data collection, is that silicon causes less

background X-ray diffraction. Fig. 3 shows the X-ray diffractograms of an empty 10  $\mu\text{m}$  CryoLoop from Hampton Research (Fig. 3a) and an empty silicon microshovel (Fig. 3b). The sizes of the fabricated microshovels range from 50 to 280  $\mu\text{m}$  in length, from 7 to 40  $\mu\text{m}$  in height and are 300  $\mu\text{m}$  in width, because these dimensions cover the expected range of protein crystal sizes we would manipulate. The square notches at the bottom of the tool stem (Fig. 1a) encode the shape and the size of the tip so that the microshovels can be easily distinguished by eye or by an automatic reading device.

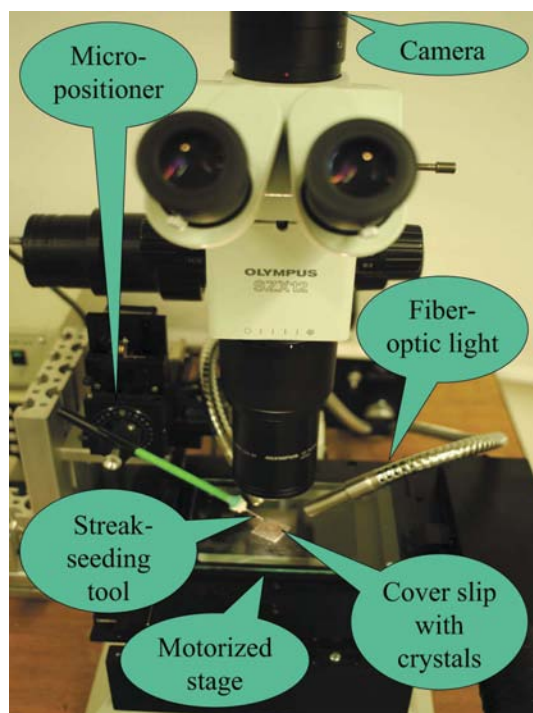


**Figure 4**  
The CARESS prototype workstation for protein crystal streak-seeding.

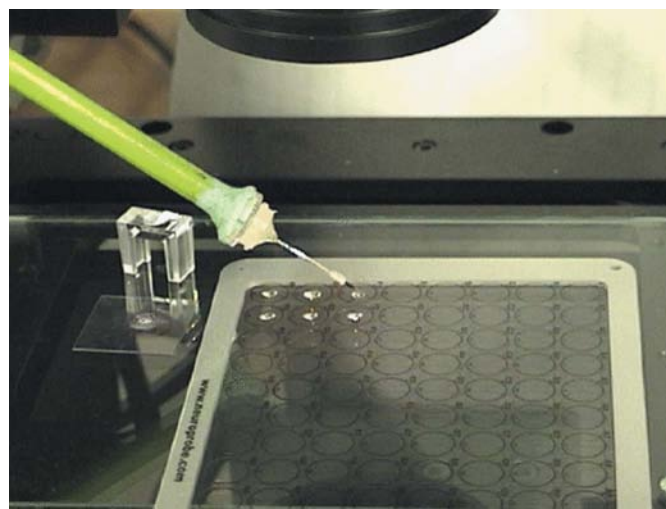


**Figure 5**  
An example showing streak-seeding of six droplets on a 96-well Neuroprobe plate coversheet. Shown on the left is a droplet with the source crystals on a 22 mm plastic cover slip. The microbridge behind it contains water for cleaning the tool.

The manufacturing process began with transferring the CAD design onto a  $100 \times 100$  mm quartz photomask. Front-side photo-lithography was then performed on a silicon wafer, part No. 4A01-20DSP/300 obtained from Montco Silicon Technologies Inc. [double-side polish, orientation  $\langle 100 \rangle$ ,  $100 \pm 0.5$  mm in diameter and a thickness (which translated to the tool width) of  $300 \pm 25$   $\mu\text{m}$ ]. The wafer was coated with AZ4620 photoresist, spun in a centrifuge and baked to achieve a uniform coating layer of approximately 10  $\mu\text{m}$  on each side. One side (the front) was exposed to the pattern from the photomask and developed using AZ400K developer. Next, the back side of this wafer was bonded to a larger sacrificial silicon wafer (double-side polish, 150 mm diameter and 625 mm thickness) and the package was processed with deep reactive ion etching (DRIE), leaving the microtools only adherent to the larger wafer. Finally, the microshovels were detached and cleaned up from the bond and the photoresist in an acetone bath.

## 2.2. Protein purification and crystallization

Expression and purification of *Haemophilus influenzae* hypothetical protein HI1161 and *Xanthomonas campestris* hypothetical protein XCC2852 (NESG targets IR63 and XcR50, respectively) was carried out as part of the established high-throughput protein-production pipeline of the NESG using previously published methods (Acton *et al.*, 2005; Benach *et al.*, 2003; crystal structure of shikimate dehydrogenase).

Preliminary crystallization trials were performed using the hanging-drop vapor-diffusion method at 291 K using Crystal Screens 1 and 2 and the PEG/Ion Screen from Hampton Research (Laguna Hills, CA, USA). After optimization of the crystallization conditions, XCC2852 crystals useful for structure determination grew over a reservoir solution containing 1.6 M  $(\text{NH}_4)_2\text{SO}_4$ , 100 mM NaCl, 100 mM HEPES pH 6.5. In the case of HI1161, optimization involved streak-seeding from slowly forming crystal clusters. Crystals of HI1161 suitable for X-ray data collection grew over reservoir solutions containing 8–8.5% (w/v) PEG 3350, 0.2 M potassium formate. Crystals appeared in 1–3 d and grew to full size ( $\sim 100 \times 20 \times 20$   $\mu\text{m}$ ) in one week. The structures were solved using multi-wavelength anomalous diffraction, refined using standard techniques and deposited in the PDB under codes 1o0i for

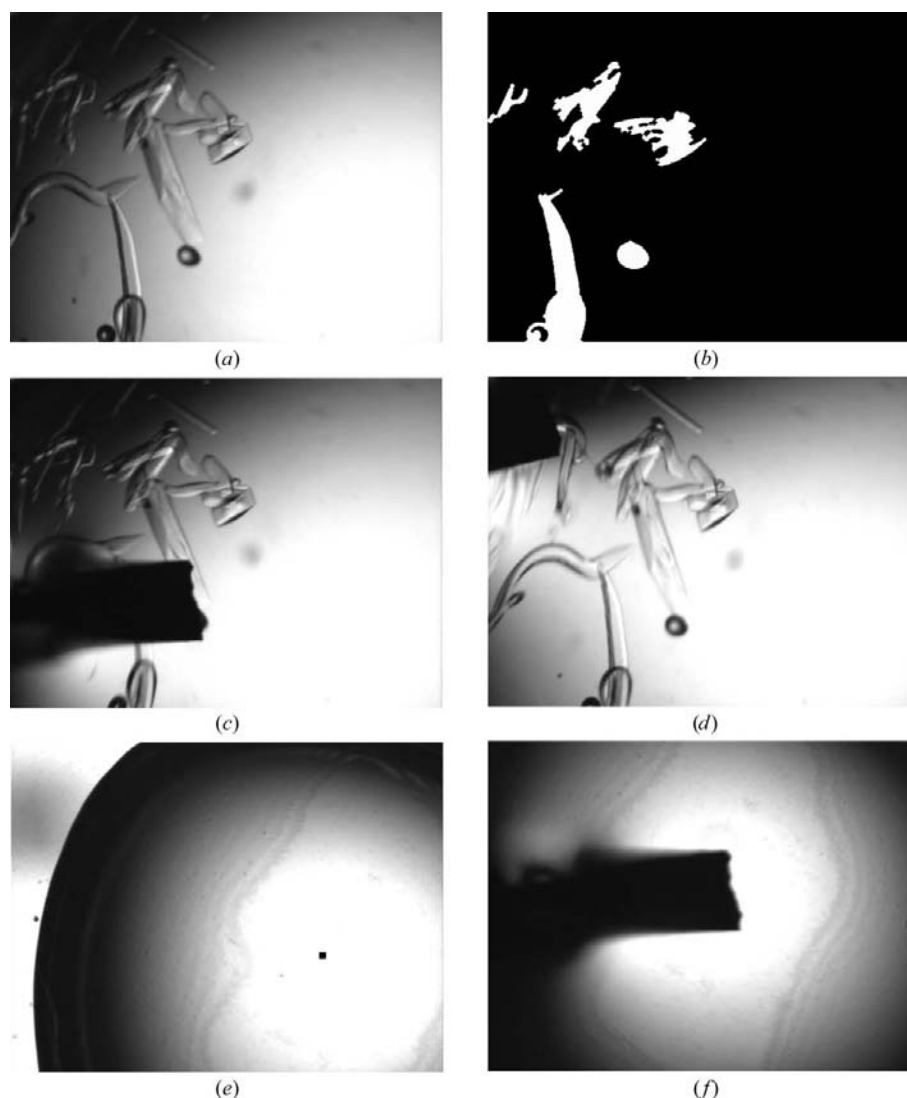


**Figure 6**

Steps of the streak-seeding procedure. (a) Initial view of the seeding crystals, (b) detected crystals (in white), (c) tool touching crystal No. 1, (d) tool touching crystal No. 2, (e) locating the center of the target droplet, (f) streaking through the target droplet.

HI1161 (1.70 Å resolution) and 1ttz for XCC2852 (2.11 Å resolution).

## 2.3. Streak-seeding robot

Traditionally, streak-seeding is a procedure that requires close human attention and that has a great deal of variability between different researchers and even between different experiments conducted by the same researcher. It also takes up valuable time of researchers, who have to perform the task manually. Because of this, our research has focused on the automation of the streak-seeding procedure. We have created a prototype robotic system, called CARESS (Columbia Automated Robotic Environment for Streak Seeding), which can autonomously perform streak-seeding on 96-well plate covers.

CARESS (Fig. 4) is based on an MP-285 micropositioner made by Sutter Instrument, Co., which is a Cartesian robot

with three degrees of freedom (DOF), a work space of approximately 16 cm<sup>3</sup> and translational resolution as good as 40 nm in each direction. The micropositioner holds and operates a streak-seeding tool (e.g. the silicon microshovels discussed earlier) as its end-effector. It has zero backlash and its fine-grain motion control is used when high positioning accuracy is needed, such as when the tool must touch small source crystals. Here, the rigidity of the silicon becomes very useful, as softer and more flexible materials would greatly reduce the positioning precision of the calibrated system. For faster and larger scale motion, we use a motorized Prior ProScan stage which has two DOF of horizontal motion and a large enough working range to process a 24-well or 96-well plate. The stage is mounted on a model SZX12 optical microscope manufactured by Olympus, which provides a total magnification of between 8.4× and 108.0× and is used to observe the work. Live video feedback of the work is captured and fed to a generic personal computer (PC) with a 2.6 GHz CPU and 1 GB RAM *via* a camera mounted on the microscope. The computer runs custom software, developed as part of the CARESS system, that processes the video stream to analyze the scene and control the motion of the micropositioner and the stage accordingly.

CARESS is currently designed to work with the hanging-drop method, seeding from source crystals in a drop on a small cover slip (e.g. 22 mm plastic cover slips for Linbro plates) to destination drops on a coversheet for a 96-well plate (e.g. by NeuroProbe Inc. or Molecular Dimensions Ltd). At the beginning of the automated streak-seeding procedure (Fig. 5), the operator places on the stage the slide with the protein crystals used as a seed source, the coversheet of the 96-well plate containing the target protein droplets where the growth of new crystals will be seeded and a microbridge with water used for cleaning the seeding tool.

The system then proceeds autonomously. Firstly, it moves the stage to position the cover slip with the source crystals under the microscope and takes an image of the crystals (Fig. 6*a*). Next, a software component identifies the locations of the crystals (Fig. 6*b*) based on an edge-detection algorithm applied to the image, followed by morphological cleaning and binary thresholding operations. The software selects two distinct positions identified as crystals and directs the tool to touch each of them (Figs. 6*c* and 6*d*). Two crystals are used in order to ensure against the rare chance of misdetection of one of them by the image-processing software. The tool descends all the way to the bottom of the drop in order to make certain that the target is touched regardless of its depth. After this, the streaking action is performed on a number of deposited protein droplets (usually an entire row) on the coversheet for the 96-well plate. The stage is moved so that each circular well cover region is consecutively centered in the field of view of the microscope. Another image-processing component locates where the protein droplet was deposited within that region (Fig. 6*e*). Finally, the tool is moved through the located droplet (Fig. 6*f*). For technical details of the image-processing components and the system, we refer the reader to Georgiev *et al.* (2005).

## 2.4. Crystallization experiments

XCC2852 crystals were used for optimization of the optical detection algorithm. The streak-seeding experiments shown below were conducted on the HI1161 protein. Different proteins were used for optimization and experiments in order to demonstrate that once set up, the system can perform on other proteins as well. Two types of experiments were performed (manual and robotic), both using the hanging-drop method.

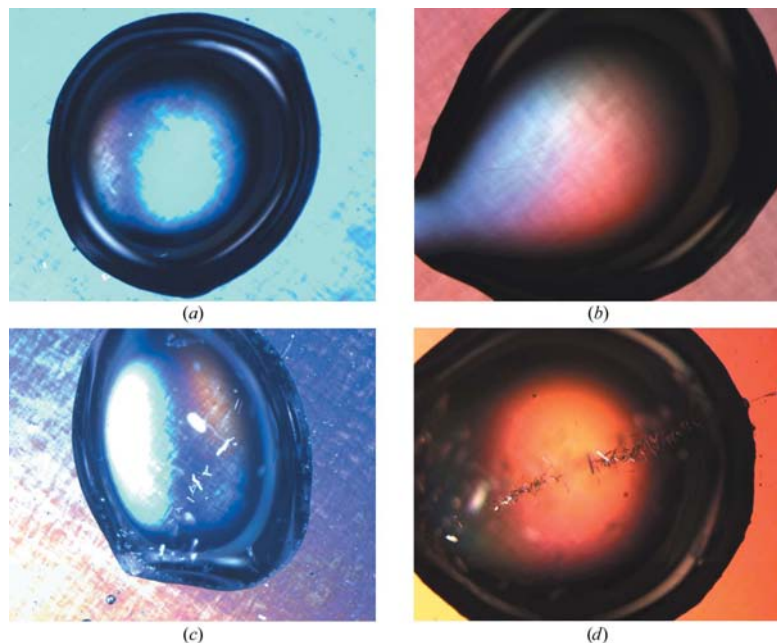
For the manual experiments, the seed source was a droplet on a 22 mm cover slip containing three-month-old HI1161 microcrystals. The plastic cover slip from the source plate was turned over to expose the microcrystals for seeding. In rapid succession, a boar bristle was touched to a source microcrystal and then streaked through a freshly prepared target droplet of protein solution mixed with an equal volume of reservoir solution on a clean air-dusted 22 mm cover slip. In a parallel operation, a silicon microshovel was touched to a different source microcrystal and then streaked through a different target droplet on the cover slip. Control droplets were prepared in an identical manner, except that no streak-seeding was performed. Additionally, identical droplets were prepared which were streaked with a clean microshovel to prove the importance of touching the pre-grown crystals. All cover slips were then flipped over on top of wells pre-filled with reservoir solution and sealed using vacuum grease to initiate hanging-drop crystallization.

For the robotic experiments, the seed sources were crystal-containing droplets on 22 mm cover slips that were grown in the same batch as those used for the manual experiments, but the target droplets were located on the surface of a Molecular Dimensions HT-96 CrystalClene coversheet. The system was set up and run as described in §2.2 above. After the robot had completed the streak-seeding, the coversheet was flipped over on top of a Greiner BioOne 96-well plate with wells pre-filled with reservoir solution. Some of the robotic experiments were run with the explicit goal of demonstrating the results obtained from serial streak-seeding. In these, a series of wells (3–8) were streaked in succession after a single loading of the microshovel with seeds.

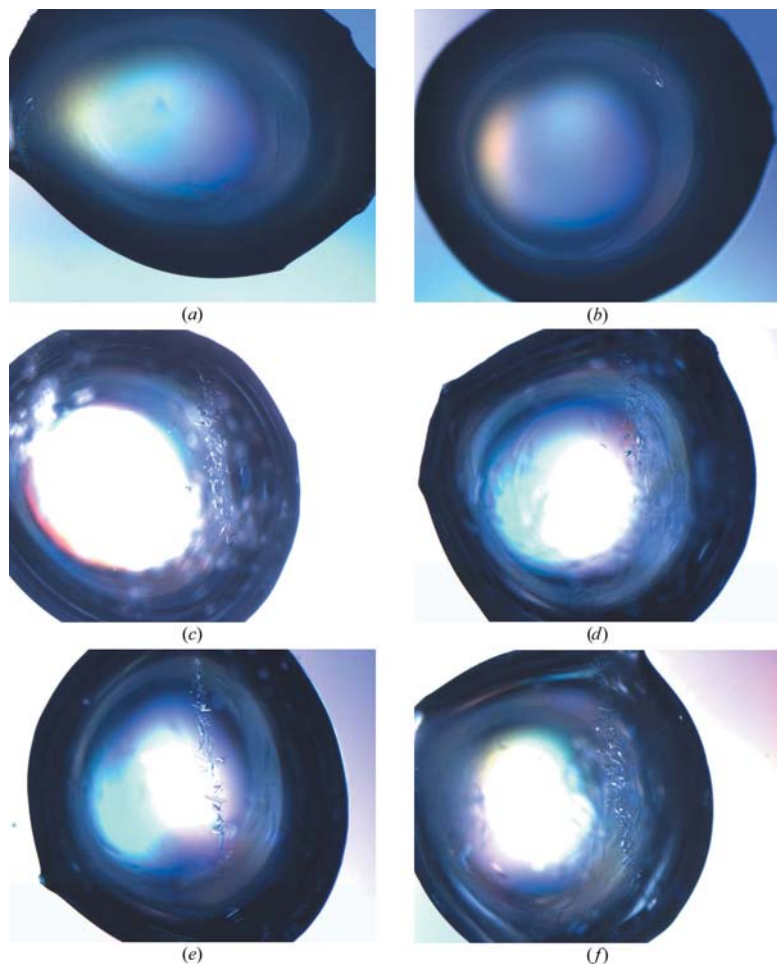
## 3. Results and discussion

Fig. 7 shows the results obtained 24 h after the manual streak-seeding experiment. No nucleation was observed in the control droplets (Fig. 7*a*) or those which were streaked with a microshovel that was not loaded with seeds (Fig. 7*b*). On the other hand, lines of microcrystals tracing the trajectory of the boar bristle (Fig. 7*c*) or the microshovel (Fig. 7*d*) were clearly visible in the seeded wells. The fact that streaking with a clean microshovel resulted in no crystals indicates that seed transfer indeed took place from the pre-grown crystals to the new droplets in the case of a loaded microshovel. No significant differences were observed between crystals seeded by a boar bristle and those seeded by a microshovel.





**Figure 7**  
Manual streak-seeding results for the HI1161 protein. (a) Control case, (b) droplet streaked with a clean microshovel, (c) droplet streaked with a loaded boar bristle, (d) droplet streaked with a loaded silicon microshovel.



**Figure 8**  
Results of the robotic streak-seeding using silicon microshovels: (a) and (b) show two control cases without seeding; (c)–(f) show four robotically seeded wells.

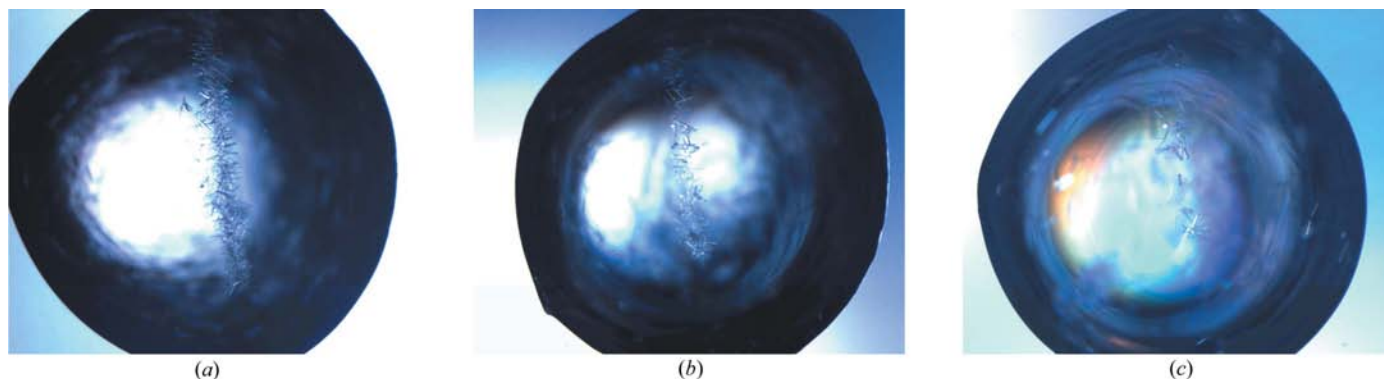
The results obtained 24 h after the seeding performed by CARESS are shown in Fig. 8. As in the case of manual seeding, no nucleation was observed in the control droplets (Figs. 8*a* and 8*b*). Figs. 8(*c*)–8(*f*) show droplets with microcrystals growing after robotic seeding. In an experiment designed to assess the repeatability of the system, 16 out of 16 wells were successfully seeded and none of the four control wells contained crystals.

Fig. 9 shows the results of a serial streak-seeding experiment performed by CARESS. The three wells in this figure were seeded in sequence from Fig. 9(*a*) to Fig. 9(*c*). It can be seen that the size of the crystals increases as their number decreases in each consecutive well. Therefore, CARESS can perform serial streak-seeding and this is one effective method for controlling the number of resulting crystals. CARESS is also well suited to consistently employ other such methods suggested in the literature, including variation of the contact-surface area of the tool or angle (Stura & Wilson, 1990). An interesting problem for further research is to quantify the effect of the variation of these and other parameters (*e.g.* streaking speed, roughness) of the microshovels on the quality of the results. The fabrication process allows great flexibility and microtools of different shape, size, thickness and surface roughness can be made just as easily and tested to empirically determine the optimum set of parameters for the given task.

The system's processing speed is currently about 6.5 wells per minute. Speed has not been optimized, because this first prototype is a proof-of-concept implementation aimed at demonstrating that a fully automated instrument can perform the procedure accurately and reproducibly. In the next iteration of the system, we are working to increase the performance by using faster hardware and optimizing the motion control. We believe that with proper hardware and optimization, the new system will be able to achieve about 300% speed improvement and process an entire 96-well plate in approximately 5 min. For the future, we are further planning to outfit the system with liquid-dispensing capabilities so that the deposition of the protein droplets on the plate cover sheet is also performed automatically to reduce dehydration during setup.

#### 4. Conclusions

An automatic approach to streak-seeding has been presented based on using novel silicon-made microshovels in place of the traditional tools such as various types of hairs, whiskers or bristles. A fabrication process for the microshovels has been developed which is based on MEMS technology and allows great flexibility in the design in terms of both



**Figure 9**  
Serial streak-seeding results: (a), (b) and (c) show three wells seeded in sequence.

shape and size. It has been demonstrated that the silicon microshovels produce comparable results to boar bristles when used for streak-seeding. Finally, a robotic prototype system has been presented which is based on the microshovels and is capable of streak-seeding 96-well plates, demonstrating the viability of this streak-seeding technology.

This work was supported by grants to the Northeast Structural Genomics Consortium from the Protein Structure Initiative of the National Institutes of Health (NIGMS-P50-GM62413 and NIGMS-U54-GM074958). We would like to thank Phillip Manor for his assistance and Gaetano Montelione, Thomas Acton and Rong Xiao for providing protein samples.

## References

- Acton, T. B. *et al.* (2005). *Methods Enzymol.* **394**, 210–243.
- Benach, J., Lee, I., Edstrom, W., Kuzin, A. P., Chiang, Y., Acton, T. B., Montelione, G. T. & Hunt, J. F. (2003). *J. Biol. Chem.* **278**, 19176–19182.
- Bergfors, T. (2003). *J. Struct. Biol.* **142**, 66–71.
- Chayen, N. E. & Saridakis, E. (2002). *Acta Cryst.* **D58**, 921–927.
- D'Arcy, A., MacSweeney, A. & Haber, A. (2003). *Acta Cryst.* **D59**, 1343–1346.
- Georgiev, A., Allen, P. K. & Edstrom, W. (2004). *Proceedings of IEEE/RSJ International Conference on Intelligent Robots and Systems*, pp. 236–241. Los Alamitos, CA, USA: IEEE.
- Georgiev, A., Allen, P., Song, T., Laine, A., Edstrom, W. & Hunt, J. F. (2005). *Robotics: Science and Systems Conference*, pp. 137–143. <http://www.roboticsconference.org>.
- Lesley, S. A. & Wilson, I. A. (2005). *J. Struct. Funct. Genomics*, **6**, 71–79.
- Saitoh, K., Kawabata, K., Kunimitsu, S., Asama, H. & Mishima, T. (2004). *Proceedings of IEEE/RSJ International Conference on Intelligent Robots and Systems*, pp. 2725–2730. Los Alamitos, CA, USA: IEEE.
- Stura, E. A. (1999). *Protein Crystallization: Techniques, Strategies and Tips*, edited by T. M. Bergfors, pp. 139–154. La Jolla, CA, USA: International University Line.
- Stura, E. A. & Wilson, I. A. (1990). *Methods*, **1**, 38–49.
- Xu, G., Chiu, C., Angelini, E. D. & Laine, A. F. (2006). In *Proceedings of the 28th Annual Conference of the IEEE Engineering in Medicine and Biology Society*. Los Alamitos, CA, USA: IEEE.
- Wang, Y., Kim, D. H., Angelini, E. D. & Laine, A. F. (2005). *SPIE International Symposium, Medical Imaging 2005: Image Processing*, 266–273. Bellingham, WA, USA: SPIE.
- Willcox, B. E., Thomas, L. M., Chapman, T. L., Heikema, A. P., West, A. P. Jr & Bjorkman, P. J. (2002). *BMC Struct. Biol.* **2**, 6–15.